Quantitative analysis of the flexibility effect of cisplatin on circular DNA

Chao Ji, Lingyun Zhang,* and Peng-Ye Wang†
Key Laboratory of Soft Matter Physics, Beijing National Laboratory for Condensed Matter Physics, Institute of Physics, Chinese Academy of Sciences, Beijing 100190, China
(Received 3 April 2013; revised manuscript received 15 September 2013; published 10 October 2013)

We study the effects of cisplatin on the circular configuration of DNA using atomic force microscopy (AFM) and observe that the DNA gradually transforms to a complex configuration with an intersection and interwound structures from a circlelike structure. An algorithm is developed to extract the configuration profiles of circular DNA from AFM images and the radius of gyration is used to describe the flexibility of circular DNA. The quantitative analysis of the circular DNA demonstrates that the radius of gyration gradually decreases and two processes on the change of flexibility of circular DNA are found as the cisplatin concentration increases. Furthermore, a model is proposed and discussed to explain the mechanism for understanding the complicated interaction between DNA and cisplatin.

DOI: 10.1103/PhysRevE.88.042703 PACS number(s): 87.14.gk, 87.64.Dz, 87.10.Pq

I. INTRODUCTION

Cisplatin is one of the most widely used anticancer drugs and is particularly useful for the treatment of testicular, ovarian, head and neck, and small-cell lung cancers [1]. It is generally believed that DNA molecules are the most important intracellular target for anticancer Pt drugs [2–4]. In an aqueous solution, two water molecules or hydroxide ions take the place of the two chloride ions from the central platinum, transforming cisplatin to an active state [5–8]. The DNA-cisplatin compound can interfere with cellular proteins by means of inhibiting transcription factors, blocking DNA polymerase or RNA polymerase functions [9,10]. The reactivity of cisplatin with DNA as an anticancer agent plays an important role in understanding biological effects of cisplatin on DNA.

The study of interactions between DNA molecules and some small molecules using atomic force microscopy (AFM) has become an interesting and significant field [11,12]. The configuration of DNA molecules ranging from hundreds to thousands of base pairs (bp) can be observed with AFM [13]. Atomic force microscopy images can clearly reveal the topological and tertiary structure of circular DNA molecules. Several topological structures of circular DNA have been reported in the contact mode or tapping mode in air and liquid environments [11,14–20]. However, the interaction between cisplatin and DNA is a complex process that can be influenced by the concentration of cisplatin, the state of cisplatin, the DNA sequence, and the reaction time. So far, little quantitative information about the configuration modifications due to the interaction between circular DNA and cisplatin has been reported.

In this study, we aim to quantitatively study the influence of cisplatin on the flexibility of DNA. In the cell nucleus, the DNA molecule is spatially confined by nucleosomes, thus the changes of flexibility introduced by cisplatin binding to DNA molecules cannot be accurately demonstrated by means of linear DNA. So in comparison with linear DNA, the circular DNA can be better to reveal the flexibility changes affected by cisplatin *in vitro*. The flexibility of linear DNA can be measured using the contour length and end-to-end distance based on AFM image processing [21,22]. However, this approach cannot be applied to the quantitative analysis of circular DNA. To resolve this issue, we used the radius of gyration to describe the changes in flexibility of circular DNA. To analyze DNA circles with complicated configurations from AFM images, a method was developed to measure the configuration and flexibility changes of circular DNA under the influence of different concentrations of cisplatin. The experimental results have been that the radius of gyration gradually decreases as the cisplatin concentration increases. A hypothesis is proposed to reveal the physical mechanism of these complicated interactions between DNA and cisplatin.

II. EXPERIMENT

A. Materials and methods

Cisplatin was purchased from Sigma-Aldrich (St. Louis, MO, USA) and converted into an aqueous derivative by reacting it with two equivalents of $AgNO_3$ in solution at room temperature for 24 h in the dark. The mixture was then centrifuged at 13 000 rpm for 10 min twice to remove the AgCl precipitate [21]. In our experiments, we used pUC19 DNA (New England Biolabs), which is a small double-stranded circular DNA molecule that is 2686 bp in length.

B. The AFM sample preparation

The following experiment was conducted to study the configuration modifications of circular DNA in the presence of cisplatin. All reactions were performed in a solution of 10-mM Tris-HCl, *p*H 7.5, and the concentration of DNA was 0.12 ng/μl. A total volume of 80 μl of reaction buffer containing pUC19 DNA and reactive cisplatin at different concentrations was incubated for 14 h at 37 °C in the dark. The concentrations of the reactive cisplatin were 0.12, 0.25, 0.5, 1, and 2 μM. For the AFM imaging observations, we took a volume of 20 μl containing 5-mM $MgCl_2$. The mixture was deposited on the surface of freshly cleaved mica, as shown in Fig. 1(a). After waiting 15 min, the mica surface was

*lyzhang@iphy.ac.cn
†pywang@iphy.ac.cn

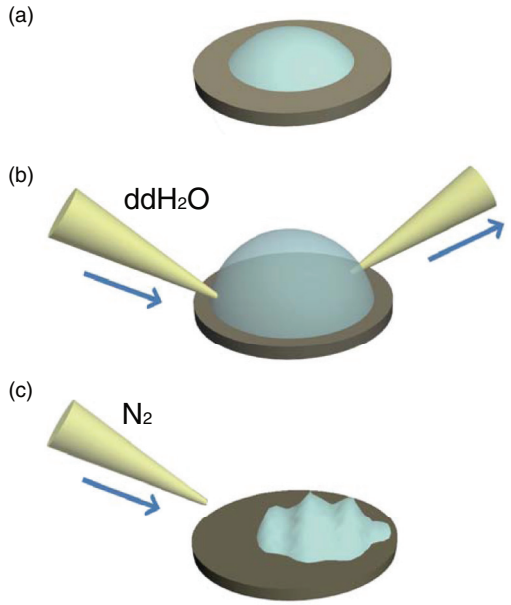

FIG. 1. (Color online) (a) A 20-μl mixture was deposited on a mica surface. (b) After 15 min, the mixture solution was washed with 200 μl of ddH_2O. (c) The sample was blown dry using a gentle stream of nitrogen gas.

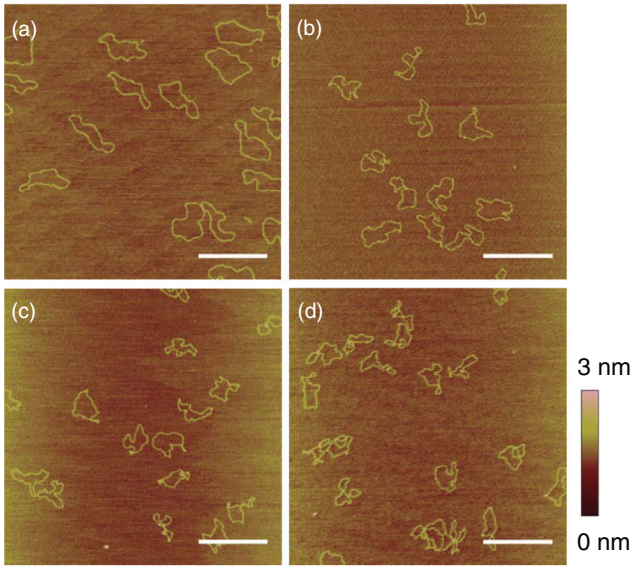

FIG. 2. (Color online) (a) The AFM images of pUC19 DNA on a mica surface. (b)–(d) The AFM images of pUC19 DNA in the presence of the following cisplatin concentrations: (b) 0.5 μM, (c) 1 μM, and (d) 2 μM. The white scale bar is 500 nm for all images.

washed several times with 200-μl Milli-Q filtered ultrapure water [Fig. 1(b)]. Finally, the aqueous solution was blown dry using a gentle stream of nitrogen gas, as shown in Fig. 1(c) [22].

C. Atomic force microscopy

In this study, all images were obtained under ambient air conditions using a multimode AFM with a nanoscopeIIIa controller (Digital Instruments, Santa Barbara, CA, USA) in tapping mode. A silicon probe (RTESP14) purchased from Veeco (USA) with a resonance frequency of 314–316 kHz was used. An E scanner was used in our experiment. The scan frequency was 1 Hz per line and the scan size was 1–4 μm. All AFM images were obtained at a resolution of 512 × 512 pixels and were not modified except for flattening.

III. RESULTS AND DISCUSSION

A. The AFM observation of circular DNA in the presence of cisplatin

The interaction between circular DNA and different concentrations of cisplatin was studied using AFM. The samples were not affected by the utilized slats [23]. Thus the configuration changes in circular DNA can be distinguished by morphology. The AFM images of pUC19 DNA in the absence of cisplatin are shown in Fig. 2(a). In general, it is difficult to obtain full three-dimensional views of the equilibrium configuration of DNA in solution. However, under the appropriate conditions, DNA adheres to a mica surface weakly enough that unlike mica modified by (3-aminopropyl)triethoxysilane, the DNA-mica interactions modified by Mg^{2+} are believed not to affect the equilibrium configurations of DNA molecules in two-dimensional views [24]. For a circular chain molecule that is 2868 bp in length, the excluded volume effects resulting from the interactions between different molecules or among segments of the same molecule are stronger on a two-dimensional surface [25]; therefore, the images of pUC19 DNA without cisplatin are circles without intersection and interwound configurations due to excluded volume effects.

The AFM images of pUC19 DNA in the presence of different concentrations of cisplatin are shown in Figs. 2(b)–2(d). As the cisplatin concentration increased, the configuration modifications of pUC19 DNA became extraordinarily obvious. The bend angles of the circular DNA were significantly increased along with the concentration of cisplatin. We found that the circular DNA were almost in circlelike forms in Fig. 2(a), but a number of kinks and some intersection structures appeared in the presence of cisplatin, as shown in Fig. 2(b). As shown in Fig. 2(c), the bend angle increased further and several intersection structures appeared. There were also some interwound structures in the presence of 1-μM cisplatin. Figure 2(d) shows an increase in the number of intersection and interwound configurations. The AFM images reveal that the configuration of pUC19 DNA in the presence of cisplatin becomes complicated and the bend angle is obviously increased.

To quantitatively analyze the change of DNA configurations, an algorithm (as demonstrated in Fig. 7) had been developed. With the aid of algorithm, DNA configurations can be classified into three kinds of structures, including circlelike, intersection, and interwound structures. The quantitative results shown in Fig. 3 suggest that the configuration of pUC19 DNA became complex with the increase of cisplatin concentration, which is indicated in the pUC19 DNA configuration in Table I. In comparison with native pUC19 DNA, the weight of the intersection structure significantly increased and the interwound structure can be observed in the presence of cisplatin.

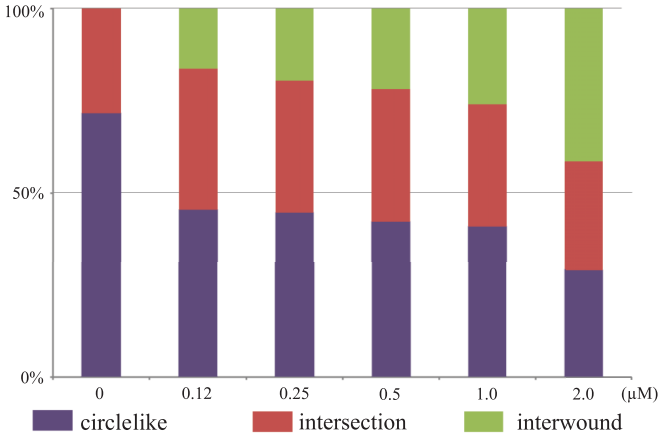

FIG. 3. (Color online) Weight of DNA configurations, including circlelike, intersection, and interwound structures, at the following concentrations of cisplatin: 0, 0.12, 0.25, 0.5, 1.0, and 2.0 μM, respectively.

B. Quantitative analysis of the flexibility of circular DNA in the presence of cisplatin

An image processing technique is developed that recognizes DNA fragments and extracts the molecular profiles from the images shown in Fig. 4(a) under varying image conditions and different molecular configurations. To extract geometrical information from AFM images, every DNA molecule must be recognized and processed through a set of image processing steps. All image processing codes are developed. The image processing is composed of the following steps.

The first step is the threshold processing that transforms the color image into a binary image. Thus those pixels that represent DNA fragments are labeled 1 and the pixels that represent the background are labeled 0 in the binary image. Second, the pixels that represent DNA fragments are preserved in a binary image. Then the thinning step removes spare pixels from each fragment and keeps the skeleton backbone of the DNA molecules to extract the correct profile, as shown in Fig. 4(b). The next step is to prune the spare branches of the skeleton that are the result of impurities in the sample, dragging of the cantilever tip, or noise close to the fragments that were not removed in the previous processing steps, as shown in Fig. 4(c). These image processing steps were used to optimize the images. Finally, the DNA molecules are extracted from the image and their coordinates are stored in different data files. The following algorithm is used. (i) The step size between two adjacent points is 4 nm. In Fig. 4(e), the current point as the initial position X_{n-1} is placed 4 nm from the other current point X_n, which is the center of the circle. (ii) The intersection point between this circle and the original skeleton is referred to as X_{n+1}. (iii) The trial point X_{n+1} is defined as the center of a new circle shown in Fig. 4(f) and the previous center X_n becomes the new initial point. (iv) Steps (i)–(iii) are repeated and the positions of the centers are stored in coordinate text files. This process is repeated until the end of the chain is reached. In the AFM images, each DNA molecular fragment is described as a chain of points determined by our image processing (but with human supervision). Successive points are separated by 4 nm, as shown in Fig. 4(d). The position information for the points is stored in different files for subsequent data analysis.

TABLE I. Quantitative result of DNA configurations.

Concentration (μM)	Circlelike (No.)	Intersection (No.)	Interwound (No.)	Ratio (%)
0	411	161	0	72:28:0
0.12	210	177	75	45:38:17
0.25	231	186	102	45:36:19
0.5	190	163	99	42:36:22
1.0	206	166	136	41:33:26
2.0	134	137	192	29:30:41

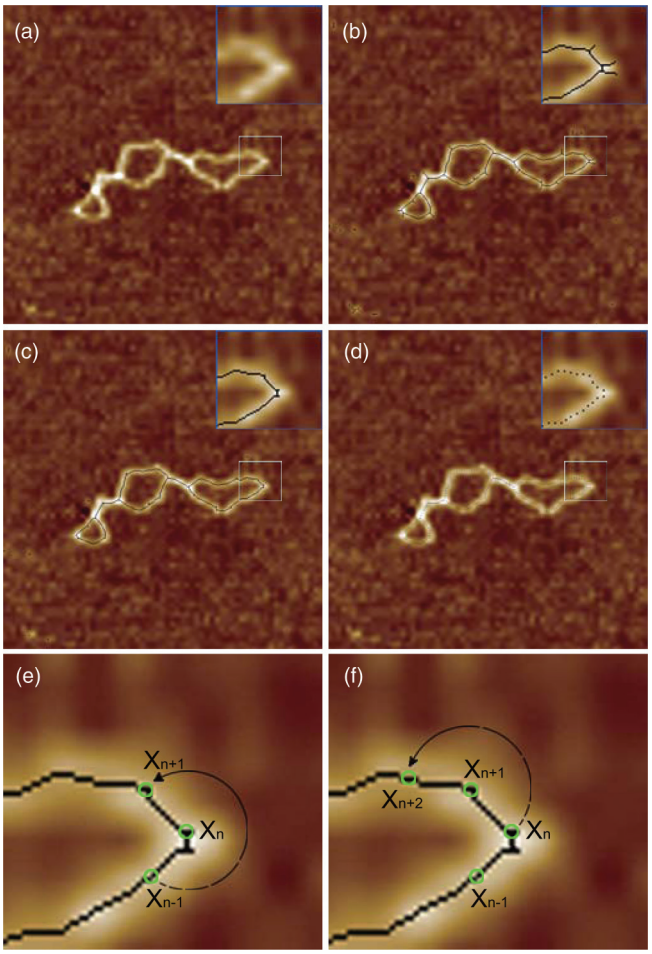

FIG. 4. (Color online) (a) Original AFM images of a single circular DNA molecule. (b) The thinning process was performed to extract the configuration profile of the DNA molecule. (c) The skeleton backbone of the DNA molecule was obtained using a pruning process. (d) The configuration of the DNA molecule was expressed by successive points tracing the skeleton backbone. (e) The new point X_{n+1} was found using the initial point X_{n-1} and the center X_n of a circle. (f) The next new point X_{n+2} was also found using the new initial point X_n and the new center X_{n+1}.

The flexibility is important for studying the physical properties of DNA in cellular processes. The flexibility of linear DNA has been measured using magnetic tweezers and AFM in the presence of cisplatin [19,26]. However, it is more valuable to measure the flexibility of circular DNA

TABLE II. Radius of gyration of pUC19 DNA for three samples. Here SD denotes standard deviation.

Cisplatin (μM)	No. (DNA)	Mean (nm)	SD (nm)	Total mean (nm)	SD of total mean (nm)
	165	114.13009	10.6881		
0	217	112.7339	10.83332	113.00381	1.01851
	190	112.14743	10.8885		
	147	101.07864	12.63551		
0.12	153	99.02129	12.61101	99.99187	1.03359
	162	99.87568	12.51928		
	148	97.70631	12.51928		
0.25	198	97.88823	11.73885	97.30165	0.86324
	173	96.31042	12.06844		
	129	97.85219	11.29804		
0.5	172	96.65982	10.3402	96.91743	0.83626
	151	96.24028	10.96129		
	192	93.99407	12.76202		
1	145	92.94512	12.53613	93.7521	0.71729
	171	94.31711	12.50354		
	155	88.07237	10.58939		
2	173	87.35975	10.33578	88.12304	0.78985
	135	88.937	9.61654		

for understanding the physical properties of DNA *in vivo*. Therefore, to obtain quantitative information and describe DNA flexibility from AFM images, we used the radius of gyration to analyze the changes in flexibility of circular DNA in the presence of cisplatin (Table II).

The radius of gyration R_g about a given axis can be measured in terms of the mass moment of inertia I around that axis and the total mass m. Thus it can be defined as $R_g = \sqrt{I/m}$. Here the DNA molecule is examined using discrete polymer models to express the flexibility of DNA. The radius of gyration discussed in polymer physics is usually understood as a mean over all polymer molecules within the sample and is measured as an ensemble

$$R_g^2 = \frac{1}{N}\sum_{k=1}^{N}(\mathbf{r}_k - \mathbf{r}_{\text{mean}})^2, \tag{1}$$

where $\mathbf{r}_{\text{mean}}$ is the mean position of the monomeric polymers.

As shown in Fig. 4(d), the pUC19 DNA fragment can be extracted to successive points traced on the skeleton backbone of every DNA molecule, thus the successive points expressed to the centers of every discrete polymers of DNA. According to Eq. (1), we can calculate the radius of gyration. The radius of gyration $\langle R_g \rangle$ of pUC19 DNA plotted against the concentrations of cisplatin is shown in Fig. 5. When repulsive interactions among segments become stronger, the value of the radius of gyration will also be bigger, which means a weakness of the flexibility effect of the DNA molecule. In contrast, a weakness of the interaction between segments results in the decrease of the radius of gyration and the formation of coiling of DNA molecules. The radius of gyration is approximately 112.94 nm in the absence of cisplatin. The radius of gyration of pUC19 DNA gradually decreases with increasing concentrations of cisplatin.

Figure 5 shows the curve of the radius of gyration versus cisplatin concentration. In the lower cisplatin concentration

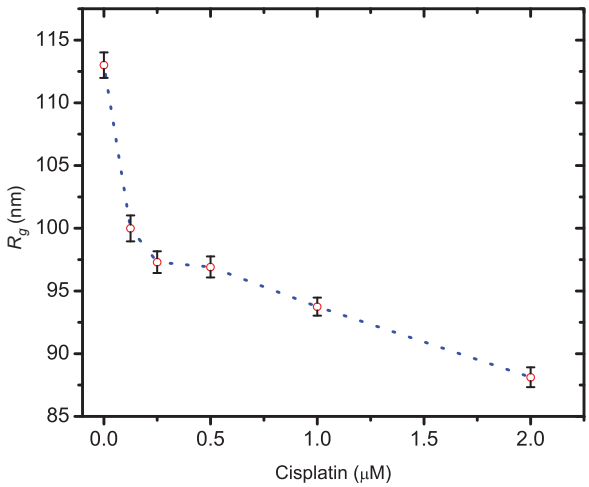

FIG. 5. (Color online) Radius of gyration of pUC19 DNA plotted against the cisplatin concentration curve. The error bar is the standard deviation of means for independent samples ($n = 3$).

(less than 0.25 μM), the radius of gyration quickly decreases with the increase of cisplatin. However, the radius of gyration smoothly changes in the higher cisplatin concentration. It is obvious that there are two processes, including a faster and a slower one.

Based on these experimental and quantitative results, we propose a hypothesis for the physics mechanism. In solution, the two chloride ions dissociate from the central platinum and two water molecules or hydroxide ions locate there as shown in Fig. 6(a). Then the platinum cations approach the DNA molecule. The water ligand can be replaced by the N7 atoms of guanine or adenine. The binding of cisplatin to the purines of the neighboring bases at two sites form the diadduct. Circular DNA can be bent and the stack structure of DNA helix can be destroyed [27]. Diadducts are formed to increase the DNA flexibility, which leads to a compact configuration of circular DNA. It is possible to produce the negative high slope of the curve (faster process) in the lower concentration as shown in Fig. 5. After the binding sites of diadducts in this DNA molecule are completely formed, the flexibility of DNA will not be obviously changed, but the decreasing trends still occur. In addition, the aqueous cisplatin can be regarded as a divalent cation in solution. Due to the electrostatic properties of cisplatin, they can bind to the surfaces of DNA molecules and neutralize DNA charges that lead to weakness of electrostatic repulsion among DNA segments [28].

In order to clearly demonstrate that the radius of gyration changes with the concentration of cisplatin in Fig. 5, two possible impact factors of the cisplatin that influence the configuration of circular DNA in solution can be considered in a reasonable way: The first factor is that cisplatin as a diadduct binds to circular DNA to result in the formation of kinks and the second factor is that cisplatin as a divalent cation possibly leads to the weakness of electrostatic repulsion on circular DNA. Its physics mechanism in the hypothesis is illustrated in Fig. 6(b). In the lower concentration of cisplatin, we infer that the diadduct effect of cisplatin can play a main role that causes a faster process. In the higher concentration, the divalent cation may plays the key role that the electrostatic repulsion is

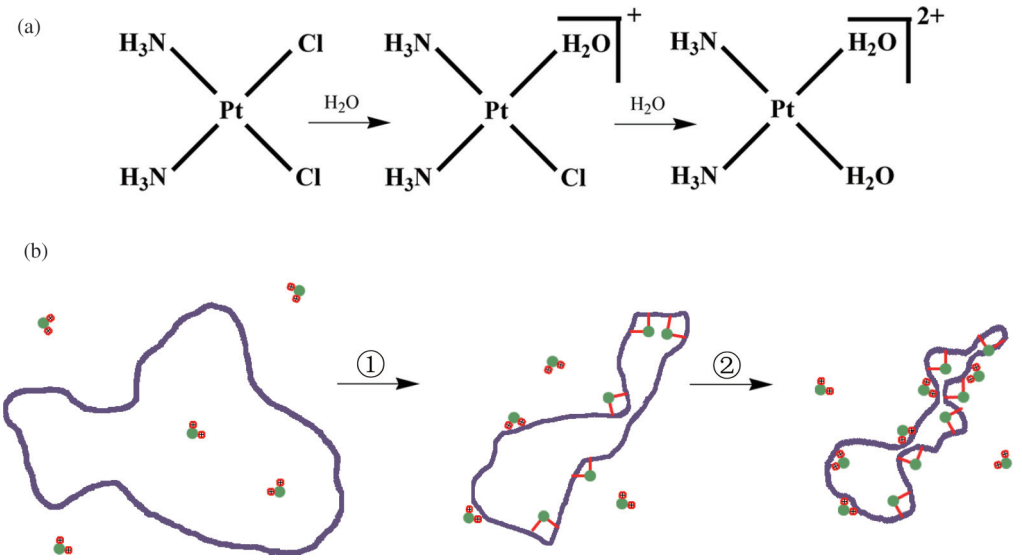

FIG. 6. (Color online) (a) Aquatic chemistry of cisplatin in solution. (b) Two possible factors of aqueous cisplatin influence the configuration of circular DNA in solution: (1) the cisplatin as a diadduct binds on circular DNA to result in the formation of kinks and (2) cisplatin as a divalent cation may leads to weakness of electrostatic repulsion on circular DNA.

decreased and leads to the flexibility of circular DNA slightly increasing.

IV. CONCLUSION

In summary, we have developed a set of methods to process AFM images for the purpose of quantitatively studying the changes in flexibility of circular DNA cisplatin. We observed that the configuration of pUC19 DNA gradually changes from a circlelike configuration to a complex configuration with intersection and interwound structures in the presence of cisplatin. The experimental results indicate that the flexibility of circular DNA is significantly increased in the presence of cisplatin. We presented an algorithm to illustrate the configuration by using the radius of gyration that was used to describe the flexibility of circular DNA. The possible physics mechanism was discussed to explain these results. There are two possible effects of the cisplatin including the binding on the DNA as a diadduct and electrostatic interaction as a divalent cation; however, the possible explanation should be tested in further studies. Our quantitative analysis of AFM images promises to be an important method for understanding the complicated interaction between DNA and cisplatin.

ACKNOWLEDGMENTS

This research was supported by the National Natural Science Foundation of China (Grant No. 11274374) and the National Basic Research Program of China (973 Program) (Grant No. 2009CB930704).

APPENDIX: CLASSIFICATION ALGORITHM OF DNA CONFIGURATIONS

The algorithm is developed to classify the configuration aspect of circular DNA molecules. A detailed description of Fig. 7 is demonstrated as follows.

(i) The point of the DNA skeleton is regarded as the center marked by A of Fig. 7(b), and the neighbor points of this center can be respectively scanned in clockwise and counterclockwise directions as shown in Fig. 7(a).

(ii) In Fig. 7(b), the value of the point through the counterclockwise direction is 1, as shown by B, and then the second point scanned in the clockwise direction until the value of the point is also 1, as shown by B′.

(iii) We can obtain position B and position B′. If the position B is equal to the position B′, as shown in Fig. 7(b), the next point will be a new center. Step (i) will be started again. If the position B is not equal to the position B′ as shown in Fig. 7(c),

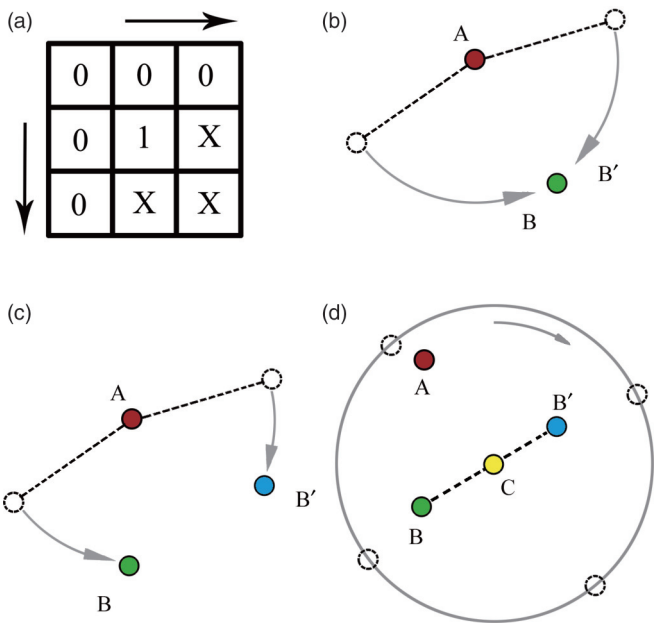

FIG. 7. (Color online) Schematic diagram of the algorithm recognizing aspects of the DNA configurations.

the position C can be calculated by the average of positions of B and B′, which is shown in Fig. 7(d).

(iv) When the point C is regarded as a new circle center, the algorithm can scan the value of points on the designated radius, so we can record the positions of intersections between the DNA skeleton and this circle, as shown in Fig. 7(d). The information of the intersections can be counted and then their relative distances calculated. If the number of intersections is less than 4, this structure is an interwound structure. Otherwise, this structure is an intersection structure.

[1] S. G. Chaney, S. L. Campbell, B. Temple, E. Bassett, Y. Wu, and M. Faldu, J. Inorg. Biochem. **98**, 1551 (2004).

[2] B. Rosenberg, L. Van Camp, J. E. Trosko, and V. H. Mansour, Nature (London) **222**, 385 (1969).

[3] J. Reedijk, Chem. Rev. **99**, 2499 (1999).

[4] E. R. Jamieson and S. J. Lippard, Chem. Rev. **99**, 2467 (1999).

[5] S. J. Lippard, Science **218**, 1075 (1982).

[6] S. L. Bruhn, J. H. Toney, and S. J. Lippard, Prog. Inorg. Chem. **38**, 477 (1990).

[7] D. P. Bancroft, C. A. Lepre, and S. J. Lippard, J. Am. Chem. Soc. **112**, 6860 (1990).

[8] N. P. Johnson, J. D. Hoeschele, and R. O. Rahn, Chem. Biol. Interact. **30**, 151 (1980).

[9] A. Vaisman and S. G. Chaney, J. Biol. Chem. **275**, 13017 (2000).

[10] Y. W. Jung and S. J. Lippard, J. Biol. Chem. **278**, 52084 (2003).

[11] G. B. Onoa and V. Moreno, Int. J. Pharm. **245**, 55 (2002).

[12] J. Ruiz, N. Cutillas, C. Vicente, M. D. Villa, G. Lopez, J. Lorenzo, F. X. Aviles, V. Moreno, and D. Bautista, Inorg. Chem. **44**, 7365 (2005).

[13] H. G. Hansma, A. L. Weisenhorn, A. B. Edmundson, H. E. Gaub, and P. K. Hansma, Clin. Chem. **37**, 1497 (1991).

[14] B. Samori, C. Nigro, A. Gordano, I. Muzzalupo, and C. Quagliariello, Angew. Chem. Int. Ed. Engl. **35**, 529 (1996).

[15] B. Samori, G. Siligardi, C. Quagliariello, A. L. Weisenhorn, J. Vesenka, and C. J. Bustamante, Proc. Natl. Acad. Sci. USA **90**, 3598 (1993).

[16] C. Ji, L.-Y. Zhang, X.-M. Hou, S.-X. Dou, and P.-Y. Wang, Chin. Phys. Lett. **28**, 068702 (2011).

[17] E. Amat, M. J. Prieto, and V. Moreno, Int. J. Pharm. **270**, 75 (2004).

[18] G. B. Onoa, G. Cervantes, V. Moreno, and M. J. Prieto, Nucleic Acids Res. **26**, 1473 (1998).

[19] X.-M. Hou, X.-H. Zhang, K.-J. Wei, C. Ji, S.-X. Dou, W.-C. Wang, M. Li, and P.-Y. Wang, Nucl. Acids Res. **37**, 1400 (2009).

[20] Z. G. Liu, S. N. Tan, Y. G. Zu, Y. J. Fu, R. H. Meng, and Z. M. Xing, Micron **41**, 833 (2010).

[21] M. Wei, S. M. Cohen, A. P. Silverman, and S. J. Lippard, J. Biol. Chem. **276**, 38774 (2001).

[22] M. J. Allen, E. M. Bradbury, and R. Balhorn, Nucl. Acids Res. **25**, 2221 (1997).

[23] W. H. Han, S. M. Lindsay, M. Dlakic, and R. E. Harrington, Nature (London) **386**, 563 (1997).

[24] G. Zuccheri, R. T. Dame, M. Aquila, I. Muzzalupo, and B. Samori, Appl. Phys. A **66**, S585 (1998).

[25] C. Rivetti, M. Guthold, and C. Bustamante, J. Mol. Biol. **264**, 919 (1996).

[26] R. Garcia and R. Perez, Surf. Sci. Rep. **47**, 197 (2002).

[27] W. Li, Z. Q. Sun, P. Xie, S. X. Dou, W. C. Wang, and P. Y. Wang, Phys. Rev. E **85**, 021918 (2012).

[28] V. B. Teif and K. Bohinc, Prog. Biophys. Mol. Biol. **105**, 208 (2011).